

Supplemental Data

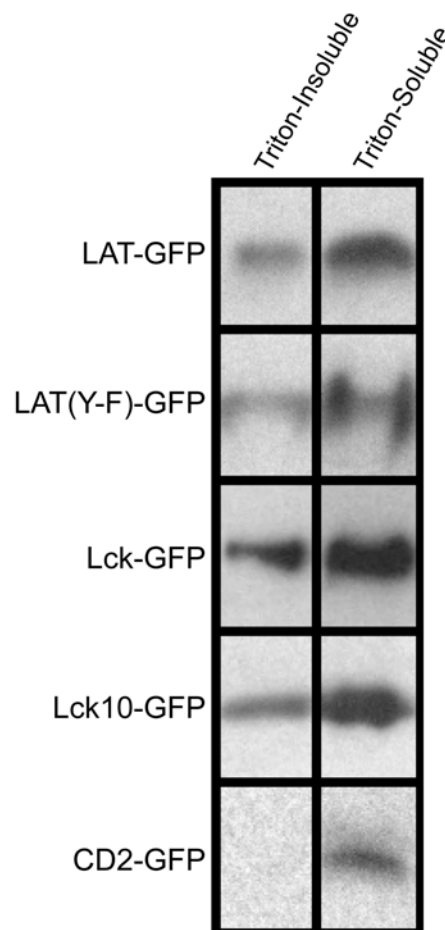
Single Molecule Microscopy Reveals Plasma Membrane

Microdomains Created by Protein-Protein Networks

that Exclude or Trap Signaling Molecules in T Cells

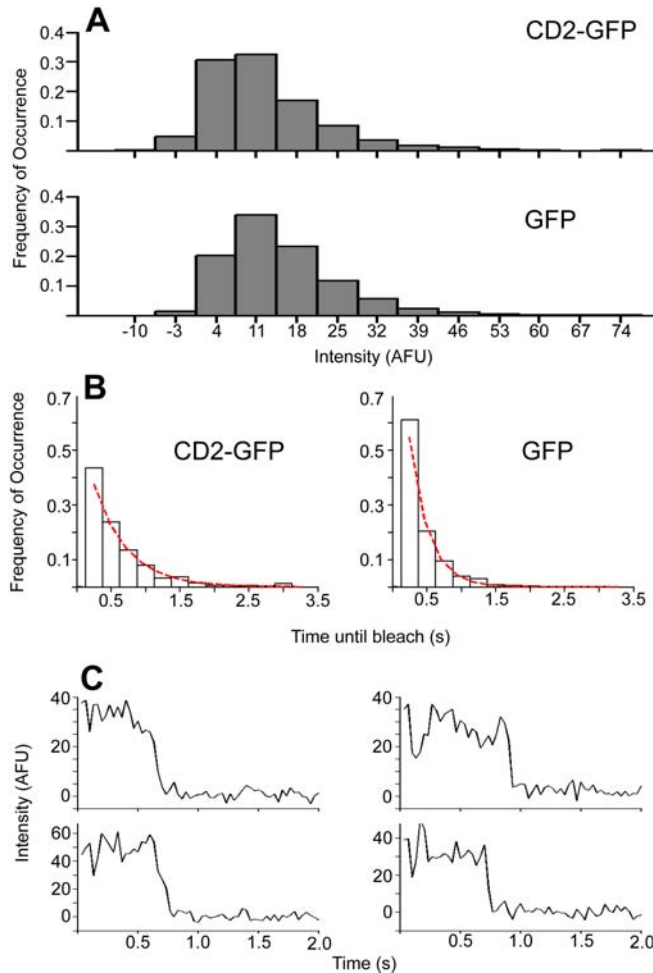
Adam D. Douglass and Ronald D. Vale

Figure S1. GFP Fusion Proteins Retain the Detergent Solubility or Insolubility of the Untagged Proteins
Supplementary Figure 1, Douglass and Vale



Jurkat cells were transfected with various GFP constructs and were allowed to recover overnight. 5×10^7 cells per construct were lysed in 0.5% Triton X-100 and fractionated on a discontinuous sucrose gradient as described elsewhere (Lin et al., 1999). Equilibrated gradients were fractionated starting at the top, and portions of each fraction were separated by PAGE, immobilized on nitrocellulose, and probed using an antibody against GFP (JL-8, Clontech). Shown are the Triton X-100 soluble (fraction 12) and insoluble (fraction 3 or 4) peaks of each gradient.

Figure S2. Discrete Fluorescent Spots in TIRF Image Series Represent single, GFP-Tagged Proteins
 Supplementary Figure 2, Douglass and Vale



Jurkat cells expressing CD2-GFP were activated on anti-TCR-coated coverslips and imaged at 37° C. After obtaining several video-rate movies of CD2-GFP diffusion, a purified GFP with an added 10 a.a. linker at the N-terminus was added to the dish at a concentration of 1 nM. Purified GFP molecules adhered to the glass between the cells and were imaged at video rate.

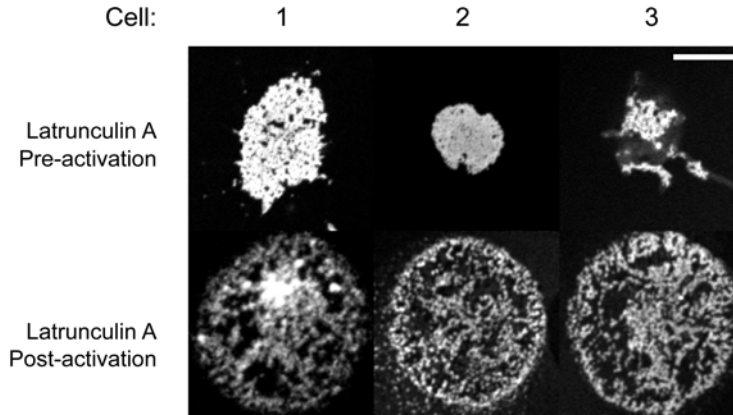
(A) The intensities of single fluorescent spots in CD2-GFP-expressing cells closely match those of GFP. The background-subtracted intensities of discrete spots in either the cell surface (CD2-GFP) or on the glass (GFP) were measured and the resulting distributions were normalized to the total number of observations. CD2-GFP, mean = 12.39; GFP, mean = 15.11 AFU (arbitrary fluorescence units). The slightly lower value for CD2-GFP is consistent with the evanescent wave decaying in intensity at greater distances from the coverslip. In both cases, a small number of negative values resulted from background subtraction.

(B) CD2-GFP particles exhibit single-step photobleaching. Background-subtracted intensities for four representative particles are plotted over time.

(C) Distributions of single-spot photobleaching times for both CD2-GFP and GFP. The distributions are well fit by single exponential functions (superimposed in red). Differences between the corresponding decay constants (CD2-GFP, $t_{0.5} = 0.42$ s; GFP, $t_{0.5} = 0.27$ s) are also indicative of dimmer illumination for cellular CD2-GFP. Particles visible for less than three frames were ignored in order to minimize the effect of transiently bound GFP. The intensities (A), single-step photobleaching (B), and single exponential decay kinetics (C) all argue that single molecules are being imaged in living cells. The close match in exponential decay constants for CD2-GFP in living cells and purified GFP argues that the disappearance of CD2-GFP is likely due to photobleaching and not to some other process, such as endocytosis.

Figure S3. The F-Actin Cytoskeleton Is Required for the Initiation, but Not Maintenance, of CD2 Clustering in Activated T Cells

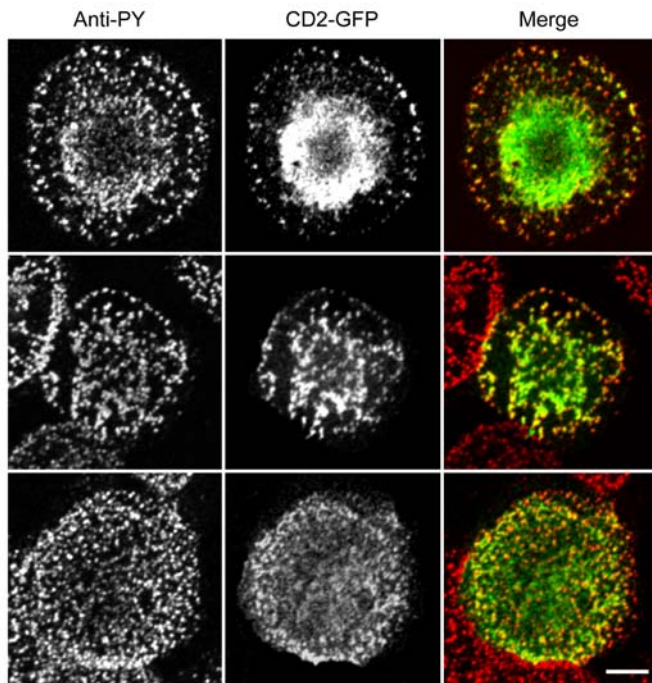
Supplementary Figure 3, Douglass and Vale



Cells were transiently transfected with CD2-GFP and 24 hr later were treated with 5 μ M Latrunculin A (Lat A) for 10 min either before or after activation by TCR crosslinking. Top, CD2 clustering and cell spreading are compromised when treated with Lat A prior to activation. Bottom, CD2 clusters remain when treated with Lat A after TCR crosslinking. Scale bar, 10 μ m.

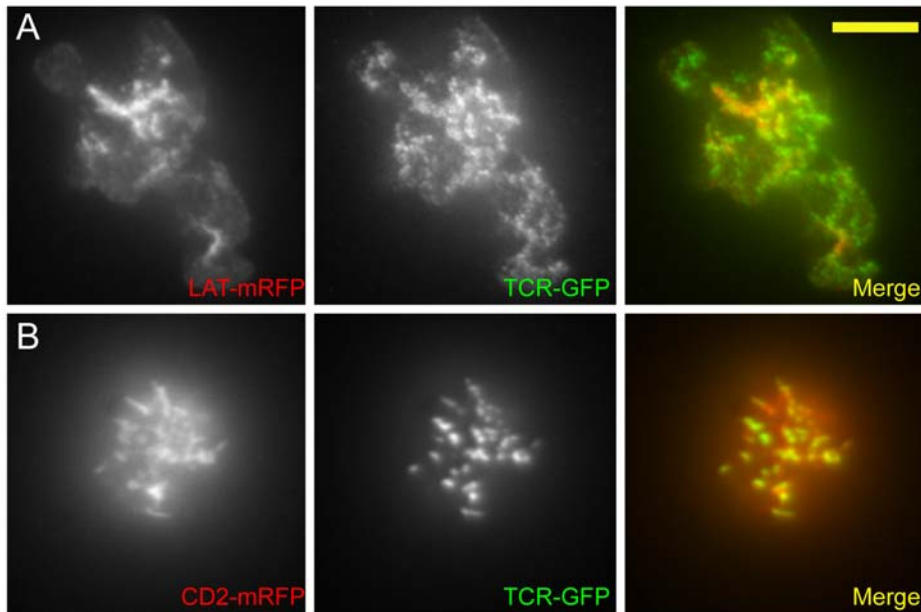
Figure S4. Colocalization of CD2-GFP with Immunofluorescence Staining from a Phosphotyrosine Antibody (Clone 4G10; anti-PY) after Applying Cells for 10 min to an Anti-TCR Surface

Supplementary Figure 4, Douglass and Vale



Scale bar, 10 μ m. The degree of overlap between these components was quantified using Pearson's correlation coefficient ($R = 0.6 \pm 0.3$), and found to be significantly different from the value of zero that would be expected for independent distributions ($p < 0.01$, t-test).

Figure S5. Temporal Variation in the Degree of Overlap between CD2 Zone Components and the TCR
Supplementary Figure 5, Douglass and Vale



Cells expressing LAT-mRFP and TCR-GFP (A) or TCR-GFP and CD2-mRFP (B) were fixed and imaged after 2 min of stimulation. These experiments partially reconcile differences between our study and that of Bunnell et al. (2002), who reported complete colocalization between LAT and the TCR at early stages of TCR signaling (0-2 min), followed by the disappearance of LAT clusters. In our experiments, LAT clusters are stable at 10 min and show a high degree of colocalization with CD2; however CD2 and the TCR show a small offset at this time point (Fig. 3). At the early time point tested here, both CD2 and LAT show good overlap with the TCR, in agreement with Bunnell et al. Thus, the subtle differences between our studies appear to reside in patterns at later time points. This might be due to differences in the method used to coat the glass surface with antibody. Bunnell et al. cleaned coverslips with a mixture of HCl and ethanol for 5 min, pre-coated the glass with poly-DL-lysine, and incubated with antibody for 3 hr before use. We cleaned coverslips with a mixture of sulfuric acid and hydrogen peroxide for three days, followed by antibody coating without the addition of poly-DL-lysine. The exact differences caused by these treatments remain to be resolved.

Supplemental References

Lin, J., Weiss, A., and Finco, T.S. (1999). Localization of LAT in glycolipid-enriched microdomains is required for T cell activation. *J. Biol. Chem.* 274, 28861–28864.

Bunnell, S.C., Hong, D.I., Kardon, J.R., Yamazaki, T., McGlade, C.J., Barr, V.A., and Samelson, L.E. (2002). T cell receptor ligation induces the formation of dynamically regulated signaling assemblies. *J. Cell Biol.* 158, 1263–1275.

Table S1. Effects of TCR Activation on Single-Molecule Diffusion Behavior

Construct	D_{rest} ($\mu\text{m}^2/\text{s}$)	D_{act} ($\mu\text{m}^2/\text{s}$)	$D_{\text{act}}/D_{\text{rest}}$	p value
LAT	0.29 ± 0.07	0.12 ± 0.02	0.41 ± 0.04	< 0.025
LAT(C-S)	0.31 ± 0.05	0.20 ± 0.04	0.65 ± 0.03	< 0.005
LAT(Y-F)	0.44 ± 0.08	0.50 ± 0.11	1.15 ± 0.20	—
Lck	0.40 ± 0.04	0.45 ± 0.02	1.15 ± 0.17	—
Lck10	0.73 ± 0.20	0.79 ± 0.2	1.10 ± 0.06	—
CD45	0.51 ± 0.13	0.51 ± 0.02	1.05 ± 0.24	—
CD2	0.04 ± 0.03	0.09 ± 0.07	1.27 ± 0.40	—

Each construct was imaged in unstimulated and activated cells on the same day to control for any variability associated with culture or other conditions. The $D_{\text{act}} / D_{\text{rest}}$ ratio was calculated for unstimulated and activated cells analyzed on the same day. The mean and standard error shown were derived from two independent experiments on separate days (three for LAT(C-S) and LAT(Y-F)). Measurements were made from 4-10 cells (total of 90-200 molecules). Significance was determined using a t-test comparison between the experimental ratio and a value of one.
